Title: "Genetic and chemical disruption of Amyloid Precursor Protein processing impairs zebrafish sleep maintenance"

Güliz Gürel Özcan[1], Sumi Lim[1], Jason Rihel [1, 2]

[1] Department of Cell and Developmental Biology, University College London, London, United Kingdom

[2] Corresponding author: j.rihel@ucl.ac.uk

Abstract:

Sleep-wake disturbances are among the earliest symptoms of Alzheimer's disease (AD) and contribute to disease severity. Since a major driver of AD—the accumulation of amyloid-beta (Aβ) in the brain—is modulated by sleep, a "vicious" feedforward cycle has been proposed in which Aβ buildup disrupts sleep, leading to more Aβ secretion and further worsening of sleep and AD. Consistent with this idea, mouse models of AD develop early sleep phenotypes, and sleep is acutely modulated by exogenous Aβ. However, these overexpression paradigms leave unclear whether endogenous Aβ signaling contributes to sleep regulation. To tackle this question, we generated loss of function mutations in the zebrafish orthologs of Amyloid Precursor Protein (APP) and monitored larval sleep behavior. Larvae with mutations in *appa* had reduced waking activity levels but normal sleep patterns, while larvae that lacked *appb* had reduced sleep due to an inability to maintain sleep bout durations. In addition, larvae exposed to the γ-secretase inhibitor DAPT, which inhibits Aβ production from APP, also have shorter sleep bouts at night. Although γ-secretase inhibition impacts the proteolytic cleavage of many proteins, *appb* mutants were insensitive to the sleep bout shortening effects of DAPT, suggesting that loss of

1

γ-secretase dependent proteolytic cleavage products of Appb are responsible for the reduced sleep maintenance phenotypes. These results are consistent with a model in which endogenous Aβ directly modulates sleep in zebrafish and supports the idea that sleep disturbances may be a useful early-onset biomarker for AD.

Introduction:

Sleep disruptions are common features of many neuropsychiatric and neurodegenerative disorders, but disrupted sleep patterns may nevertheless play a causative role in the development or progression of disease. For example, patients with Alzheimer's Disease (AD) have reductions in the amount of rapid eye movement (REM) and non-REM (NREM) sleep, an increase in the amount of wakefulness, more sleep fragmentation (Allen et al., 1987; Loewenstein et al., 1982; Prinz et al., 1982; Vitiello et al., 1990), and electroencephalographic (EEG) alterations in sleep features (D'Atri et al., 2021), yet these symptoms occur many years before cognitive decline and cell death (Sterniczuk et al., 2013). Healthy young men (~22 years old) with high genome-wide polygenic risk scores for AD have higher slow wave energy during sleep (Muto et al., 2021). Similarly, both excessive daytime sleepiness and high sleep fragmentation in cognitively normal adults are associated with increased risk of Aβ deposition (Spira et al., 2018) and AD, respectively (Lim et al., 2013). Finally, daytime napping might reduce AD risk (Anderson et al., 2021).These observations suggest that alterations in sleep may not only be an early biomarker for AD but also that sleep disruption may alter the course of the disease.

One way by which sleep may contribute to the progression of AD is via modulation of the extracellular accumulation of the two major toxic proteins of AD, Amyloid-β (Aβ) and Tau. During normal sleep-wake cycles, Aβ and Tau levels in the brain interstitial fluid (ISF) and cerebrospinal fluid (CSF) increase during wake and decrease during sleep (Holth et al., 2019; Ju et al., 2017; Kang et al., 2009; Zhao et al., 2019). This cycle is likely driven by wake-active neuronal activity, as the generation and release of Aβ and Tau into the ISF is controlled by electrical and synaptic activity (Bero et al., 2011; Cirrito et al., 2005; Kamenetz et al., 2003); however, the increased clearance of toxic material from the brain during sleep may also contribute to this rhythmic dynamic (Xie et al., 2013). Consistent with this view, experimental modulation of sleep alters Aβ release. For example, one night of sleep deprivation in humans significantly increased detectable Aβ levels in the brain (Shokri-Kojori et al., 2018), slow-wave sleep disruption increased Aβ levels in the CSF (Ju et al., 2017), and chronic sleep restriction in mouse AD models (Kang et al., 2009) or rats (Zhao et al., 2019) increased Aβ plaque accumulation. Conversely, pharmacologically or optogenetically improving sleep in mouse models of AD reduced the overall lifetime Aβ plaque burden (Jagirdar et al., 2021; Kang et al., 2009). Together, these observations have led to the proposal that sleep and Aβ dynamics create a positive feedforward cycle, wherein increases in wakefulness result in increased extracellular Aβ and aggregation, which then dysregulates sleep, further exacerbating the creation of pathogenic Aβ production (Ju et al., 2014; Roh et al., 2012).

Much less clear in this formulation is how the sleep and wake-dependent accumulation of Aβ in turn disrupts sleep, but AD-related cell death of critical sleep/wake regulatory neurons has been proposed as a possible mechanism

(Fronczek et al., 2012; Lim et al., 2014; Manaye et al., 2013). However, sleep symptoms in AD patients often appear before cognitive impairment (Sterniczuk et al., 2013), and at least some transgenic AD mouse models show disrupted sleep phenotypes preceding plaque burden (Huitron-Resendiz et al., 2002; Jyoti et al., 2010; Kollarik et al., 2021; Platt et al., 2011; Roh et al., 2012; Sterniczuk et al., 2010; Wang et al., 2002), even in the absence of neuronal loss (Colby-Milley et al., 2015; Irizarry et al., 1997; Sethi et al., 2015). An alternative hypothesis is that Aβ itself acts as a signalling molecule to modulate sleep and that this normal sleep regulatory process is disrupted in AD progression by changes in Aβ oligomeric state or plaque formation. We have previously shown in zebrafish that Aβ size-dependently and reversibly modulates sleep and wakefulness without cell death via two molecularly distinct pathways including the Prion Protein (PrP)-mGluR5-Fyn kinase signalling cascade (Ozcan et al., 2020). Acute application of Aβ oligomers in rodents also modulates sleep in a PrP dependent manner (Del Gallo et al., 2021). However, these experiments used exogenously applied Aβ, while animal models of AD overexpress multiple mutant copies of the Amyloid beta precursor protein (APP), leaving open the question as to whether Aβ plays an endogenous role in sleep regulation.

To address this question, we made loss of function mutations of the two orthologs of the human APP gene in zebrafish, *appa* and *appb*, and assessed their sleep and wake behaviour using a high throughput behavioural assay (Rihel et al., 2010). Zebrafish have the complete repertoire of App processing machinery, including an α-secretase (ADAM10)(Huxley-Jones et al., 2007), two β-secretase proteins (BACE-1 and 2) (van Bebber et al., 2013), and the proteins to build the γ-secretase complex, including Presenilin-1 (PSEN-1), Presenilin-2 (PSEN-2), Presenilin enhancer 2

(PEN-2), APH1 (anterior pharynx-defective 1), and Nicastrin (NCSTN) (Francis et al., 2002; Groth et al., 2002; Leimer et al., 1999; Sager et al., 2010). While the mammalian APP gene encodes multiple protein isoforms that are distinctly expressed and preferentially processed into specific cleavage products, in zebrafish the major Aβ-producing proteins are encoded by two genes, allowing us to experimentally tease apart isoform-specific phenotypes. Here, we show that loss-of-function $appa^{\Delta5/\Delta5}$ and $appb^{-/-}$ mutants have different sleep and activity phenotypes. By combining genetic analysis with pharmacological manipulation of the γ-secretase dependent cleavage of APP into Aβ, we further demonstrate that a short sleeping phenotype of $appb^{-/-}$ is likely due to the loss of γ-secretase dependent proteolytic fragments of Appb. Together, our experiments are consistent with a physiological role for App/Aβ in regulating sleep maintenance in zebrafish.

RESULTS

Generating *appa* and *appb* mutants

There are two *App* genes in zebrafish, *appa* and *appb*, which raises the question whether they have redundant functions. We first examined their relationship to the human APP isoforms, because gene duplications often take on isoform or tissue specific roles (Pasquier et al., 2016). Zebrafish Appa is more similar to the KPI-domain containing APP751 and 770 isoforms that predominate in non-neuronal tissues (Nalivaeva and Turner, 2013; Tanzi et al., 1988; Weidemann et al., 1989), while the Appb protein lacks the KPI domain and is more similar to the neuronally enriched and more amyloidogenic human isoform, APP695 (Kang et al., 1987;

Weidemann et al., 1989) (Figure 1A and C). Both Appa and Appb have respectively an 80% and 71% conserved identity in the Aβ42 region compared to human APP, with conserved proteolytic cleavage sites (Figure 1B). Similar to the human isoform APP695, the *appb* gene is more abundantly expressed in the zebrafish brain than *appa*, although both are detected there (Figure1D). *appb* is also highly expressed in the very early stages of zebrafish development (Figure 1E). Together, the gene expression patterns and structural homology differences of zebrafish Appa and Appb are consistent with these proteins possibly having specific functions.

To investigate the role of *app* in sleep, we generated deletions in both the *appa* and the *appb* genes in zebrafish. To isolate mutations in *appa*, we used CRISPR/Cas9 (Hwang et al., 2013). The CRISPR design tool CHOPCHOP (http://chopchop.cbu.uib.no) was used to identify candidate gRNAs to target the conserved Aβ region (amino acid residues 25-35) of *appa* (Montague et al., 2014), which was then co-injected with Cas9 into zebrafish eggs at the one cell-stage. Injected animals (F0s) that harbored frameshift mutations were then identified by Illumina sequencing and outcrossed to wild type animals to generate mutant families (see Methods). One family was isolated that harbors a 5 base pair frameshift deletion (*appa$^{\Delta 5}$*) that leads to an early stop codon within the Aβ domain. The *appa$^{\Delta 5}$* allele therefore lacks the conserved residues 26-42 of the Aβ and the entire intracellular C-terminus of Appa (Figure 1B, C).

To generate a loss of function mutation in the *appb* gene, two Transcription activator-like effector nuclease (TALEN) arms targeting a conserved region within the first exon of the zebrafish *appb* gene were designed using the Zifit software (http://zifit.partners.org/ZiFiT/) (Sander et al., 2007). These TALEN arms were each fused to one half of a Fok1 heterodimer to generate mutagenic double strand breaks within the target site of *appb* (Figure 1C). F0 fish that had been co-injected at the one cell stage with mRNA encoding the two TALEN arms were Illumina sequenced to identify a founder that contains an *appb* allele (*appb$^{Δ14+4}$*) with a 14 base pair deletion and a 4 base pair insertion that generates a frameshift followed by an early stop codon. This founder was used to generate a stable heterozygous family (herein called *appb$^{-/+}$*) for subsequent behavior analysis (Figure 1C).

appa$^{Δ5/Δ5}$ and appb$^{Δ14+4}$ (appb$^{-/-}$) have distinct sleep-wake profiles

appa$^{Δ5/Δ5}$ mutants do not have any obvious morphological abnormalities during development, have normal survival rates to adulthood, and are generally healthy and fertile. To examine whether *appa$^{Δ5/Δ5}$* mutant larvae have sleep or wake phenotypes, we used automated video monitoring to track larvae from in-crosses of *appa$^{Δ5/+}$* parents over several days on a 14hr:10hr light:dark cycle (Figure 2). Sleep in zebrafish is defined as a period of inactivity lasting longer than one minute and is associated with an increased arousal threshold and other features of behavioral sleep including circadian and homeostatic regulation (Barlow et al., 2017). Average waking activity quantifies the movements that occur during active bouts, excluding the sleep periods. Assessing these parameters across the day and night for *appa$^{Δ5/Δ5}$* mutants and their wild type (WT) siblings uncovers subtle differences in

mutant behavior. The $appa^{\Delta 5/\Delta 5}$ mutant had a reduction of 9.0% (lower bound, -15.0%; upper bound, -3%, 95% confidence interval, CI) in waking activity during the day compared to $appa^{+/+}$ siblings (Figure 2B). At night, $appa^{\Delta 5/\Delta 5}$ mutants also trended to slightly lower waking activity levels (-4.7%, [-10.0%; -0.5%, 95%CI]) (Figure 2C). In contrast, neither the total sleep (Figure 2E-F) nor the structure of sleep such as the number and duration of sleep bouts (Supplementary Figure 2-1) were statistically different across genotypes during either the night or the day periods.

Together, these data show that neither full length Appa nor its cleavage products are required for normal sleep states in zebrafish larvae, although it influences locomotor drive during the day.

We also did not observe any obvious developmental delays or morphological abnormalities in $appb^{-/-}$ mutants and therefore assessed whether whether Appb might play a non-redundant role in larval sleep regulation. Similar to $appa^{\Delta 5/\Delta 5}$ mutants, $appb^{-/-}$ larvae had a reduction in waking activity of 13.0% [-20.2; -5.6, 95%CI] relative to $appb^{+/+}$ siblings during the day (Figure 3A, B). However, unlike $appa^{\Delta 5/\Delta 5}$ animals, which trended to have slightly less waking activity at night, $appb^{-/-}$ larvae had an increase in activity of 8.2% [3.3%; 13.0%, 95%CI] compared to wild type siblings (Figure 3C). We also observed that while $appb^{-/-}$ larvae have unaffected sleep during the day (Figure 3D, E), they had an 7.9% (-14.0; -7.0%, 95%CI) reduction in sleep at night (Figure 3F), which corresponds to ~30 min less sleep per night. Thus, both Appa and Appb regulate daytime wakefulness but have non-

overlapping roles in regulating nighttime activity and sleep, with only *appb* mutants exhibiting sleep phenotypes.

To investigate the underlying mechanism of decreased night sleep of $appb^{-/-}$ mutants, we compared the sleep architecture of these mutants to their wild type and heterozygous siblings. We specifically examined whether the change in total sleep was due to alterations in the number of sleep bouts (i.e., how often sleep is initiated) or the average sleep bout lengths (i.e., once sleep is initiated, how long it is maintained). The average sleep bout length was shorter by 12.1% (-21.2%; -3.2%, 95%CI) in $appb^{-/-}$ mutants during the day and by 14.9% (-23.9%; -5.9%, -23.9%, 95%CI) at night compared to their WT siblings (Figure 3G,H). The number of sleep bouts during either the day or night were not significantly different between $appb^{-/-}$ mutants and wild type animals (Figure 3I, J). These results show that the $appb^{-/-}$ mutants initiate sleep normally but cannot maintain continuous sleep for as long as WT, indicating a defect in sleep maintenance.

$appb^{-/-}$ and a γ-secretase inhibitor have non-additive effects on sleep.

Because App's complex proteolytic cleavage makes it impossible to distinguish which peptides might be modulating sleep, we tested whether a γ-secretase inhibitor that blocks the production of Aβ phenocopies any of the sleep and wake phenotypes we observed in the *appa* and *appb* mutants. We first determined if the γ-secretase inhibitor DAPT might phenocopy *appa* or *appb* mutants. First—unlike either *appa* or *appb*, which both have reduced waking activity during the day, DAPT had no effect

9

on daytime or nighttime activity in WT animals (Figure 4A-C). This demonstrates either that the γ-secretase dependent cleavage products of App are not responsible for the effects of loss of *appa/appb* on waking activity or that DAPT's inhibition of the cleavage of other proteins counterbalance any effects from App modulation. In contrast, and similar to *appb*$^{-/-}$ animals, DAPT selectively reduced total sleep at night by -6.7% (-13.8; -0.06, %95 CI) (Figure 4F) but had no effect in the day (Figure 4D-E). As in *appb*$^{-/-}$ mutants, this nighttime reduction in sleep was due to a 14.9% reduction (-27.6; -2.7, 95% CI) in sleep bout lengths (-14.9% [-27.6; -2.7, %95 CI]) (Figure 4H) rather than the sleep bout numbers (Figure 4I-J), an effect size nearly identical to that observed in *appb*$^{-/-}$ mutants. Thus, DAPT phenocopies the nighttime sleep maintenance defects of *appb*$^{-/-}$ mutants.

Since in humans Aβ is predominantly made by the APP695 isoform (Kang et al. 1987, Weidemann et al., 1989), which is most similar to zebrafish Appb, and DAPT produces a short sleeping phenotype similar to *appb*$^{-/-}$ mutants, we hypothesized that the defect in the *appb*$^{-/-}$ mutant sleep maintenance was specifically due to the lack of γ-secretase cleavage products from Appb such as Aβ. To test this idea, we reasoned that *appb*$^{-/-}$ mutants, which lack all Appb protein products, would be refractory to the sleep-bout shortening effects of DAPT. We therefore tested the effect of DAPT on *appb*$^{-/-}$ mutants and observed that DAPT has no significant effect on *appb*$^{-/-}$ sleep (Figure 5A-G, Supplementary Figure 5-1). This non-additive effect demonstrates that DAPT and *appb*$^{-/-}$ likely act in the same molecular pathway to modulate sleep bout length at night. The non-additivity can be most clearly observed in Figure 5H and 5I, where the effect of DAPT on total sleep and sleep bout length at night are replotted and normalized to simultaneously ran WT controls (same data as in Figure 4), revealing a significant interaction between DAPT and *appb* genotype

(genotype x drug interaction, p<0.05 for night sleep and p=0.0015 for sleep bout length at night, two-way ANOVA). Mutants lacking *appb* have reduced and more fragmented nighttime sleep that cannot be reduced further by DAPT, as in WT animals (Figure 5H, I) We conclude that the short sleeping phenotype of *appb* mutants is therefore due to the loss of Appb-derived γ-secretase cleavage products, which include Aβ.

DISCUSSION

Comparison to other App loss of function studies

We found that both *appa* $^{Δ5/Δ5}$ and *appb*$^{-/-}$ zebrafish had reduced locomotor activity during the day, but only *appb*$^{-/-}$ animals had a reduction in sleep maintenance at night. Previous studies of mouse *App* knockouts have also observed reduced locomotor and exploratory activity, but many other phenotypes, including reduced growth and brain weight, reduced grip strength, hypersensitivity to seizures, alterations in copper and lipid homeostasis, reactive gliosis, and impaired spatial learning have been described (Dawson et al., 1999; Grimm et al., 2005; Li et al., 1996; Magara et al., 1999; Muller et al., 1994; Seabrook et al., 1999; Steinbach et al., 1998; Tremml et al., 1998; White et al., 1999; Zheng et al., 1995). However, the lack of major morphological and developmental phenotypes in both *appa* and *appb* mutants stands in stark contrast to several reports that investigated zebrafish App function with morpholino knockdowns. For example, morpholino knockdown of zebrafish Appb has variously been reported to affect convergent-extension during gastrulation (Joshi et al., 2009), axon outgrowth of spinal motor neurons (Abramsson et al., 2013; Song and Pimplikar, 2012), hindbrain neurogenesis (Banote et al., 2016), or cerebrovascular development (Luna et al., 2013). Given that our

observations are in line with other recent studies that do not find large developmental phenotypes for zebrafish *app* mutants (Banote et al., 2020; Chebli et al., 2021; Kanyo et al., 2020), together with the wildly divergent abnormalities described for morpholino knockdown of the same *appb* gene, we suggest these morpholino based observations are experimental artefacts.

Although sleep has not been investigated in zebrafish *app* mutants before, two other studies have examined the role of *appb* on larval locomotor activity, coming to different conclusions than what we draw here. One *appb* morpholino study found knockdown resulted in hyperlocomotion between 28-45 hpf (Abramsson et al., 2013), while we find both *appa*$^{\Delta5/\Delta5}$ and *appb*$^{-/-}$ larvae at older stages (4-7dpf) are less active than their wild type siblings. These contrasting results are likely due to differences in locomotor behavior regulation at different stages of development, methodological differences (morpholino vs. knockout), or both. Another study of *appb*$^{-/-}$ larvae tracked locomotor behavior for 60 minutes at a similar developmental age to our study (6 dpf) but found no differences in locomotion when comparing *appb* mutants to non-sibling wild type animals (Banote et al., 2020). Given that we found *appa* and *appb* mutants are only 8-10% less active than sibling-matched wild type animals during the day, the short, 60 min observation window may not have been sufficient to capture this difference; alternatively, the time of day of observation might affect the ability to detect locomotor phenotypes (e.g. see Figure 2A and 3A). Indeed, we found *appb* mutants were significantly more, not less, active at night (Figure 3C).

Overall, our sleep and wake analysis of *appa* and *appb* mutants are broadly consistent with other rodent and zebrafish studies and expands the known phenotypes associated with App loss of function mutations. These results also demonstrate that Appa and Appb play at least partially non-redundant roles in the regulation of sleep and locomotor activity in larval zebrafish, which may explain why the zebrafish phenotypes of single mutants are somewhat milder than that reported for rodent App knockouts.

Sleep maintenance, Appb, and Aβ

We observed no sleep phenotypes in $appa^{\Delta5/\Delta5}$ mutants, but $appb^{-/-}$ mutants had reduced nighttime sleep due to an inability to maintain longer sleep bout durations. Why do mutations in the two App orthologs in zebrafish lead to different phenotypes? One possibility is the difference in expression, as *appb* mRNA is more abundant and widespread in the larval zebrafish brain than *appa*, which may mean that specific sleep/wake circuits depend mostly on functional Appb proteins. Alternatively, since the protein structure of Appb is more similar to the mammalian APP695 isoform, the major source of Aβ in humans, while Appa is more similar to the KPI-domain containing APP770 (Figure 1 and (Musa et al., 2001)), the differential effect on sleep may be due to different propensities of Appb versus Appa to generate Aβ in zebrafish larvae. Depending on its oligomeric state, Aβ does have both sleep-promoting and inhibiting properties when injected into zebrafish larvae (Ozcan et al., 2020), engaging many areas of the brain including the sleep-promoting galanin-positive neurons of the preoptic area and hypothalamus (Reichert et al., 2019). However, in that study, exogenous application of the sleep-promoting Aβ oligomers

predominantly increased sleep bout initiation rather than disrupting sleep bout maintenance, as observed here in *appb*$^{-/-}$ mutants (Ozcan et al., 2020). This may indicate that other non-Aβ cleavage products of Appb, such as C99 or AICD are critical for endogenous sleep regulation. Alternatively, since the oligomeric state of Aβ dictates its effects on sleep and arousal in zebrafish (Ozcan et al., 2020), this discrepancy in the effects on sleep structure could be due to inevitable differences between endogenous and exogenous Aβ protein forms.

We also found that the γ-secretase inhibitor DAPT, which prevents the production of Aβ and other proteins from APP, leads to shortened sleep bouts at night. Inhibition of γ-secretase prevents the cleavage of many membrane-bound proteins in addition to APP, most notably the developmental signaling protein, Notch, which has also been implicated in regulating sleep in Drosophila (Seugnet et al, 2011). However, since *appb*$^{-/-}$ larvae were refractory to the sleep-shortening effects of DAPT (Figure 4), it is more likely that DAPT is exerting its sleep effects through the inhibition of Appb processing by γ-secretase. While this result is consistent with the idea that Aβ is an endogenous regulator of zebrafish sleep states, this data does not rule out a predominant or additional sleep-regulatory role for other App γ-secretase cleavage products such as AICD. Future studies could examine whether mutations in components of γ-secretase, such as Presenilin-1 or Presenilin-2 also have reduced sleep bout lengths. Another enzyme, β-secretase, which is also referred to as beta-site APP cleaving enzyme (BACE1), is also required for Aβ production from App. Zebrafish *bace1*$^{-/-}$ mutants have hypomyelination in the peripheral nervous system (van Bebber et al., 2013), but to date no sleep phenotypes have been described. As

we performed here for *appb* and DAPT, the examination of sleep phenotypes in *appb*^{-/-}; *bace1*^{-/-} or *presenilin1/2*[-/-] double mutants could be used to tease out which phenotypes are due to the specific cleavage of Appb.

Another possibility by which Appb could contribute to sleep regulation is raised by the recent observation that in zebrafish both Appa and Appb are colocalized to cilia and to cells lining the ventricles at 30 hours post fertilization (Chebli et al., 2021).The *appa*^{-/-}; *appb*^{-/-} double mutants had morphologically abnormal ependymal cilia and smaller brain ventricles (Chebli et al., 2021). It would be interesting to see if the localization of App proteins to cilia and ventricles are important for sleep and locomotion, as the coordinated periodic beating of the cilia is involved in the generation of CSF flow within ventricle cavities (Lechtreck et al., 2008) and CSF circulation is believed to facilitate transfer of signaling molecules and removal of metabolic waste products important for behaviour (Abbott et al., 2018; Ethell, 2014).

To conclude, we found that intact Appb processing is important for larval zebrafish to maintain longer sleep bouts at night. Given that sleep history over one's lifetime may be a significant contributor to AD risk and progression, these resμlts support the idea that disruptions to Aβ production may be a direct contributor to sleep phenotypes associated with preclinical and clinical AD. The specificity of the effect of Appb loss on sleep architecture also suggests that specific changes in sleep patterns that could serve as a useful AD biomarker may yet be discovered.

15

METHODS:

Zebrafish strains and husbandry

Zebrafish (*Danio rerio*) were raised under standard conditions at 28°C in a 14hr:10hr light:dark cycle. All zebrafish experiments and husbandry followed standard protocols of the UCL Fish Facility. *AB*, *TL and ABxTL* wild-type strains, *appa*^{Δ5} *(u539)* and *appb*$^{Δ14+4}$*(u537)* (also called *appb*$^{-/-}$ in this manuscript) were used in this study. Ethical approval for zebrafish experiments was obtained from the Home Office UK under the Animal Scientific Procedures Act 1986 under project licenses 70/7612 and PA8D4D0E5 awarded to JR and 70/24631 to GGO.

Generation of *appa* mutant: The *appa* gene was targeted by CRISPR/Cas9 mutagenesis. CHOPCHOP (http://chopchop.cbu.uib.no) was used to identify an sgRNA to *appa* (Montague et al., 2014). Cas9 mRNA was made from pT3TS-nCas9n (Addgene, plasmid 46757 (Jao et al, 2013)) using mMESSAGE mMACHINE transcription kit (Thermofisher Scientific**)**. Constant oligomer (5'AAAAGCACCGACTCGGTGCCACTTTTTCAAGTTGATAACGGACTAGCCTTATT TTAACTTGCTATTTCT AGCTCTAAAAC-3') and the *appa* gene-specific oligomer targeting the conserved 25-42 amino acid region of Aβ in *appa* (target sequence: 5'-GAGGACGTGAGCTCCAATAA- 3') were annealed on a PCR machine and filled in using T4 DNA polymerase (NEB) (Gagnon et al, 2014). The template was cleaned up using a PCR clean-up column (Qiaquick) and the product was verified on a 2% agarose gel. The sgRNA was transcribed from this DNA template using Ambion MEGAscript SP6 kit (Gagnon et al, 2014). 1 µl of Cas9 mRNA **(**200 ng/µl), and 1 µl of the purified sgRNA (25 ng/µl) were co-injected into one-cell stage embryos. Injected fish were grown into adulthood and sequenced.

Generation of *appb* null mutant: The *appb* gene was disrupted using TALEN mutagenesis (Sander et al., 2011). Two TALEN arms targeting a conserved region within the first exon of zebrafish *appb* gene were designed using the Zifit software (http://zifit.partners.org/ZiFiT/)(Figure 1C) (Sander et al., 2007) with Left Talen binding site sequence: 5'-TATGGACCGCACGGTATT-3', Right TALEN binding site sequence: 5'-CGACTTTGTCCCTCGCCA-3' and Spacer sequence: 5'-TTAATGCTGACGA-3'.

TALENs were generated using the FLASH assembly method in a 96 well plate (Reyon et al. 2013). The library consisted of 376 plasmids that encode one (α and β), two (βγ, βγ* and δε*), three (βγδ) or four (βγδε) TAL effector repeats consisting of all possible combinations of the NI, NN, HD or NG repeat variable di-residues (RVDs). The four 130 bp α-unit DNA fragments were amplified from each α-unit plasmid using the Herculase II Fusion DNA polymerase (Agilent) and oJS2581 and oJS2582 primers (Reyon et al. 2013). The resulting 5' biotinylated PCR products were digested with BsaI-HF (NEB) to generate four base-pair overhangs. To generate the DNA fragments encoding the βγδε (extension fragment) and βγδ (termination fragment) repeats, each of these plasmids was digested with BbsI followed by serial restriction digests of XbaI, BamHI-HF and SalI-HF (all NEB) to cleave the plasmid backbone. The four TALEN expression vectors encoding one of four possible RVDs were linearised with BsmBI (NEB). The biotinylated α unit fragments were ligated to the first βγδε fragments using Quick T4 DNA ligase and bound to Dynabeads MyOne C1 streptavidin-coated magnetic beads (Life Technologies). The bead bound α-βγδε fragments were digested with BsaI-HF

(NEB) to prepare the 3' end of the DNA fragments for the subsequent ligation step. Each extension and termination fragment is ligated to assemble the complete DNA fragment encoding the TALE repeat array by repeated digestion and ligation steps and a final digestion with BbsI (NEB) released the full length fragments. The purified DNA fragments were ligated into one of four BsmBI (NEB) digested TALEN expression vectors encoding one of four possible RVDs using Quick T4 DNA ligase. Ligation products were transformed into chemically competent XL-10 Gold *E. coli* cells and clones grown on LB Agar plates containing Ampicillin at 37°C overnight. Bacterial colonies of each TALEN arm were selected and screened by colony PCR using primers oSQT34 (5′-GACGGTGGCTGTCAAATACCAAGATATG-3′) and oSQT35 (5′-TCTCCTCCAGTTCACTTTTGACTAGTTGGG-3′). Clones showing a correct size band were cultured in LB medium containing Ampicillin at 37°C overnight. Following plasmid mini-preparation the inserts were sequenced using primers oSQT1 (5′-AGTAACAGCGGTAGAGGCAG-3′), oSQT3 (5′-ATTGGGCTACGATGGACTCC-3′) and oJS2980 (5′-TTAATTCAATATATTCATGAGGCAC-3′. mRNA was synthesised using the mMESSAGE mMACHINE T7 and polyA tailing kit. After injection of 1 µl of 100 pg/µl of each of the TALEN mRNAs, F0 embryos were raised to adulthood and sequenced.

Sequencing/Genotyping Pipeline:

F0 embryos were raised to adulthood, fin-clipped and deep-sequenced by Illumina Sequencing (MiSeq Reagent Nano Kit v2 (300 Cycles) (MS-103–1001)) to identify founders. Fin-clipping was done by anesthetizing the fish by immersion in 0.02%

18

MS-222 (Tricaine) at neutral pH (final concentration 168ug/ml MS-222). DNA was extracted by HotSHOT (Meeker et al., 2007) by lysing a small piece of the fin in 50 µl of base solution (25 mM KOH, 0.2 mM EDTA in water), incubated at 95°C for 30 min, then cooled to room temperature before 50 µl of neutralisation solution (40 mM Tris-HCL in water) was added. For *appa*, a 214 base pair fragment surrounding the conserved 25-35th amino acid region within *appa* was PCR amplified using gene-specific primers with miSeq adaptors (forward primer, 5'-TCGTCGGCAGCGTCAGATGTGTATAAGAGACAGCCTGCAGGAATAAAGCTGATCT-3'; reverse primer, 5'-GTCTCGTGGGCTCGGAGATGTGTATAAGAGACAGATGGACGTGTACTGCTTCTTCC-3'). The PCR program was: 95°C – 5 min, 40 cycles of [95°C – 30 s, 60°C – 30 s, 72°C – 30 s], 72°C – 10 min. For *appb,* founders were identified by PCR amplification using the primers (forward: 5' -TCGTCGGCAGCGTCAGATGTGTATAAGAGACAGCAG-CTGACTTTCCCTGGAGCA-3'; reverse: 5'-GTCTCGTGGGCTCGGAGATGTGTATAAGAGACAG-TGGAGGAGAACCAAGCTCCTTC-3'). PCR program was 95°C – 5 min, 40 cycles of [95°C – 30 s, 60°C – 30 s, 72°C – 30 s], 72°C – 10 min.

The PCR product's concentration was quantified with Qubit (dsDNA High Sensitivity Assay), then excess primers and dNTPs were removed by ExoSAP-IT (ThermoFisher) following the manufacturer's instructions. The samples were then sequenced by Illumina MiSeq to assess the presence of insertion/deletions. The mutant F0 fish containing a 5 base pair deletion in the Aβ region resulting in a stop codon on the 27th residue of Aβ was chosen to generate a stable mutant line *appa^{Δ5} (u539)*. An *appb* mutant carrier containing a 14 bp deletion and a 4 bp insertion *appb$^{Δ14+4}$ (u537)* that is predicted to generate a frameshift and early stop codon

19

was selected to make stable mutant lines for further analysis. F0 fish with indels were then outcrossed to wild-types and 10 one day old F1 embryos from each pairing were screened by Sanger sequencing to assess the nature of the mutations that passed into the germline. To minimize potential off-target mutations, mutant fish were crossed to ABxTL and TL WT strains for 3 generations before performing any behaviour experiments.

KASP genotyping

For rapid genotyping of mutant zebrafish harbouring the *appa$^{\Delta 5}$* and *appb$^{\Delta 14+4}$* alleles, a mutant allele-specific forward primer, a wild-type allele-specific forward primer and a common reverse primer were used using the KASP assay (LGC Genomics, KBS-1050-102, KASP-TF V4.0 2X Master Mix 96/384, Standard ROX (25mL)). The primer sequences were targeted against the following:

appa$^{\Delta 5}$

5'-
CTTTCTCTTTGTCTCCTGCCTTCAGGTTTTCTTTGCGGAGGACGTGAGC**[TCCAA/-]**TAAAGGAGCTATTATTGGCCTGATGGTCGGAGGCGTCGTCATAGCAACCATCATCGTCATCACGCTGGTGATGCTGAGGAAGAAGCAGTACACGTCCATCCACCACGGCATCATCGAGGTGCGTGAGTT

CACACCGTCTCCAC-3'

appb $^{\Delta 14+4}$

5'-

AAAATCGCGACAGAAAAACCCTGATCCGCTCAGGATATATATDCACCAGGACGT

GCTGCGCTTGGGAACACAGCCATGGGTATG

GACCGCACGGTATTCCTGCT**[GTTAATGCTGACGA/TTGT]**CTTTGTCCCTCGCC

ATCGAGGTAAGAATGATTGTGTAATGGAGAA

GGAGCTTGGTTCTCCTCCATACTTTAAAGGGCGGCCA-3'

where [x/-] indicates the indel difference in [WT/mutant].

Fluorescence was read on a CFX96 Touch Real-Time PCR Detection System (Bio-Rad) and the allelic discrimination plot generated using Bio-Rad CFX Manager Software.

Behavioural experiments: Behavioural tracking of larval zebrafish was performed as previously described (Prober et al., 2006; Rihel et al., 2010). Zebrafish larvae were raised on a 14hr:10hr light:dark cycle at 28.5°C and at were placed into individual wells of a square-well 96-well plate (Whatman) containing 650 μL of standard embryo water (0.3 g/L Instant Ocean, 1 mg/L methylene blue, pH 7.0) at 4-5 dpf. Locomotor activity was monitored using an automated video tracking system (Zebrabox, Viewpoint LifeSciences) in a temperature-regulated room (26.5°C) and exposed to a 14hr:10hr white light:dark schedule with constant infrared illumination

(Viewpoint Life Sciences). Larval movement was recorded using the Videotrack quantization mode. The movement of each larva was measured and duration of movement was recorded with an integration time of 60 sec. Data were processed using custom PERL and MATLAB (The Mathworks, R2019a) scripts, and statistical tests were performed using MATLAB (The Mathworks, R2019a).

Any one-minute period of inactivity was defined as one minute of sleep (Prober et al., 2006). Sleep bout length describes the duration of consecutive, uninterrupted minutes of sleep whereas sleep bout number is the number of such sleep events in a given time interval. Average waking activity represents activity only during active periods.

All mutant larval zebrafish experiments were performed on siblings from $appa^{+/\ \Delta5}$ or $appb^{+/\ \Delta14+4}$ heterozygous incrosses, except for experiments with DAPT, which were simultaneously performed on larvae from WT and $appb^{\Delta14+4/\ \Delta14+4}$ incrosses from different parents. DAPT (Cell Guidance Systems, SM15-10) was dissolved in DMSO to make a stock concentration of 10 mM and diluted further to a working concentration of 10 μM in water in 1:10 serial dilutions. 6 μl of the 10 μM DAPT stock or 6 μl of 0.1% DMSO control was added individually to the wells in the behaviour plate to make a 100 nM final concentration the second day at Zeitgeber time 0 (Lights ON) of the video-tracking in each experiment.

Zebrafish *in situ* hybridization (ISH)

RNA was extracted from 30 WT embryos (5dpf) by snap freezing in liquid nitrogen and TRIzol RNA extraction (Ambion 15596026). 1 µg of RNA was reverse transcribed with AffinityScript (Agilent, 600559) to make cDNA.

Templates for *in vitro* transcription for *appa* and *appb* were generated by PCR using a reverse primer that contains a T7 promoter sequence (*appa* forward primer: 5'-CGCGGGTAAAGAGTCTGAGAGC-3', *appa*-T7_reverse primer: 5'-TAATACGACTCACTATAGGG CAGACA GTATTCCTCCGACTC-3', APPb_F : 5'-GCTCCAGGAGATATAAACGAAC-3', APPb_T7R: 5'-TAATACGACTCACTATAGGG GCCGAACCTTTGGAATCTCGG-3' using the cDNA library. 5 dpf larvae and 1,2,4,8 cell stage embryos were fixed in 4% paraformaldehyde (PFA) (with 4% sucrose for 5 dpf larvae) overnight at 4°C, transferred into Phosphate Buffered Saline (PBS) the next morning. For 5dpf larvae, the brains were dissected by removing skin, cartilage, and eyes. A dioxigenin (DIG)-11-UTP-labeled antisense riboprobe targeting the gene transcript of interest was synthesized using the DIG labelling kit (Roche) and T7 RNA polymerase (Thisse and Thisse, 2008). Probe hybridization was carried out in hybridization buffer (50% formamide (v/v), 5x SSC (750 mM NaCl, 75 mM sodium citrate), 9.2 mM citric acid, 0.5 mg/mL Torula RNA, 0.05 mg/mL heparin, 0.1 % Tween-20) supplemented with 5% dextran sulfate overnight at 65°C. The larvae were then incubated overnight at 4°C with anti-Dig-AP (1:2000 in 5% normal goat serum, 11093274910, Roche) and washed before detecting alkaline phosphatase using NBP/BCIP(Roche) according to the manufacture's guidelines.

Statistical Tests:

Dabest estimation package was used for calculating the effect size as a bootstrap 95% confidence interval by creating multiple resamples from the dataset, and computing the effect size of interest on each of these resamples (Ho et al, 2019). The bootstrap resamples of the effect size were then used to determine the 95% CI and making the graphs (Ho et al., 2019). All statistical tests were done using MATLAB (The Mathworks, R2019a). Data was tested first for normality using the Kolmolgorov-Smirnov Normality test, outliers were removed using Grubb's test at $p<0.01$, and the data was analysed with one-way ANOVA or Kruskal-Wallis followed by Tukey's post-hoc test. A two-way ANOVA was used to calculate the interaction statistic for the DAPT x *appb* genotype.

REFERENCES:

Abbott, N.J., Pizzo, M.E., Preston, J.E., Janigro, D., Thorne, R.G., 2018. The role of brain barriers in fluid movement in the CNS: is there a 'glymphatic' system? Acta Neuropathol 135, 387-407.

Abramsson, A., Kettunen, P., Banote, R.K., Lott, E., Li, M., Arner, A., Zetterberg, H., 2013. The zebrafish amyloid precursor protein-b is required for motor neuron guidance and synapse formation. Dev Biol 381, 377-388.

Allen, S.R., Seiler, W.O., Stahelin, H.B., Spiegel, R., 1987. Seventy-two hour polygraphic and behavioral recordings of wakefulness and sleep in a hospital geriatric unit: comparison between demented and nondemented patients. Sleep 10, 143-159.

Anderson, E.L., Richmond, R.C., Jones, S.E., Hemani, G., Wade, K.H., Dashti, H.S., Lane, J.M., Wang, H., Saxena, R., Brumpton, B., Korologou-Linden, R., Nielsen, J.B., Asvold, B.O., Abecasis, G., Coulthard, E., Kyle, S.D., Beaumont, R.N., Tyrrell, J., Frayling, T.M., Munafo, M.R., Wood, A.R., Ben-Shlomo, Y., Howe, L.D., Lawlor, D.A., Weedon, M.N., Davey Smith, G., 2021. Is disrupted sleep a risk factor for Alzheimer's disease? Evidence from a two-sample Mendelian randomization analysis. Int J Epidemiol 50, 817-828.

Banote, R.K., Chebli, J., Satir, T.M., Varshney, G.K., Camacho, R., Ledin, J., Burgess, S.M., Abramsson, A., Zetterberg, H., 2020. Amyloid precursor protein-b facilitates cell adhesion during early development in zebrafish. Sci Rep 10, 10127. Banote, R.K., Edling, M., Eliassen, F., Kettunen, P., Zetterberg, H., Abramsson, A., 2016. beta-Amyloid precursor protein-b is essential for Mauthner cell development in the zebrafish in a Notch-dependent manner. Dev Biol 413, 26-38.

Barlow, I.L., Rihel, J. 2017 Zebrafish sleep: from geneZZZ to neuronZZZ. Curr Opin Neurobiol 44, 65-71

Bero, A.W., Yan, P., Roh, J.H., Cirrito, J.R., Stewart, F.R., Raichle, M.E., Lee, J.M., Holtzman, D.M., 2011. Neuronal activity regulates the regional vulnerability to amyloid-beta deposition. Nat Neurosci 14, 750-756.

Chebli, J., Rahmati, M., Lashley, T., Edeman, B., Oldfors, A., Zetterberg, H., Abramsson, A., 2021. The localization of amyloid precursor protein to ependymal cilia in vertebrates and its role in ciliogenesis and brain development in zebrafish. Sci Rep 11, 19115.

Cirrito, J.R., Yamada, K.A., Finn, M.B., Sloviter, R.S., Bales, K.R., May, P.C., Schoepp, D.D., Paul, S.M., Mennerick, S., Holtzman, D.M., 2005. Synaptic activity regulates interstitial fluid amyloid-beta levels in vivo. Neuron 48, 913-922.

Colby-Milley, J., Cavanagh, C., Jego, S., Breitner, J.C., Quirion, R., Adamantidis, A., 2015. Sleep-Wake Cycle Dysfunction in the TgCRND8 Mouse Model of Alzheimer's Disease: From Early to Advanced Pathological Stages. PLoS One 10, e0130177.

D'Atri, A., Scarpelli, S., Gorgoni, M., Truglia, I., Lauri, G., Cordone, S., Ferrara, M., Marra, C., Rossini, P.M., De Gennaro, L., 2021. EEG alterations during wake and sleep in mild cognitive impairment and Alzheimer's disease. iScience 24, 102386.

Dawson, G.R., Seabrook, G.R., Zheng, H., Smith, D.W., Graham, S., O'Dowd, G., Bowery, B.J., Boyce, S., Trumbauer, M.E., Chen, H.Y., Van der Ploeg, L.H.T.,

Sirinathsinghji, D.J.S., 1999. Age-related cognitive deficits, impaired long-term potentiation and reduction in synaptic marker density in mice lacking the beta-amyloid precursor protein. Neuroscience 90, 1-13.

Del Gallo, F., Bianchi, S., Bertani, I., Messa, M., Colombo, L., Balducci, C., Salmona, M., Imeri, L., Chiesa, R., 2021. Sleep inhibition induced by amyloid-beta oligomers is mediated by the cellular prion protein. J Sleep Res 30, e13187.

Ethell, D.W., 2014. Disruption of cerebrospinal fluid flow through the olfactory system may contribute to Alzheimer's disease pathogenesis. J Alzheimers Dis 41, 1021-1030.

Francis, R., McGrath, G., Zhang, J., Ruddy, D.A., Sym, M., Apfeld, J., Nicoll, M., Maxwell, M., Hai, B., Ellis, M.C., Parks, A.L., Xu, W., Li, J., Gurney, M., Myers, R.L., Himes, C.S., Hiebsch, R., Ruble, C., Nye, J.S., Curtis, D., 2002. aph-1 and pen-2 are required for Notch pathway signaling, gamma-secretase cleavage of betaAPP, and presenilin protein accumulation. Dev Cell 3, 85-97.

Fronczek, R., van Geest, S., Frolich, M., Overeem, S., Roelandse, F.W., Lammers, G.J., Swaab, D.F., 2012. Hypocretin (orexin) loss in Alzheimer's disease. Neurobiol Aging 33, 1642-1650.

Gagnon, J. A., Valen, E.; Thyme, S. B., Huang, P., Akhmetova, L., Pauli, A., Montague, T. G., Zimmerman, S., Richter, C., Schier, A. F. 2014 Efficient mutagenesis by Cas9 protein-mediated oligonucleotide insertion and large-scale assessment of single-guide RNAs, PLoS One, 9, e98186.

Grimm, M.O.W., Grimm, H.S., Patzold, A.J., Zinser, E.G., Halonen, R., Duering, M., Tschape, J.A., De Strooper, B., Muller, U., Shen, J., Hartmann, T., 2005. Regulation of cholesterol and sphingomyelin metabolism by amyloid-beta and presenilin. Nat Cell Biol 7, 1118-1123.

Groth, C., Nornes, S., McCarty, R., Tamme, R., Lardelli, M., 2002. Identification of a second presenilin gene in zebrafish with similarity to the human Alzheimer's disease gene presenilin2. Dev Genes Evol 212, 486-490.

Ho, J., Tumkaya, T., Aryal, S., Choi, H., Claridge-Chang, A., 2019. Moving beyond P values: data analysis with estimation graphics. Nat Methods 16, 565-566.

Holth, J.K., Fritschi, S.K., Wang, C., Pedersen, N.P., Cirrito, J.R., Mahan, T.E., Finn, M.B., Manis, M., Geerling, J.C., Fuller, P.M., Lucey, B.P., Holtzman, D.M., 2019. The sleep-wake cycle regulates brain interstitial fluid tau in mice and CSF tau in humans. Science 363, 880-884.

Huitron-Resendiz, S., Sanchez-Alavez, M., Gallegos, R., Berg, G., Crawford, E., Giacchino, J.L., Games, D., Henriksen, S.J., Criado, J.R., 2002. Age-independent and age-related deficits in visuospatial learning, sleep-wake states, thermoregulation and motor activity in PDAPP mice. Brain Res 928, 126-137.

Huxley-Jones, J., Clarke, T.K., Beck, C., Toubaris, G., Robertson, D.L., Boot-Handford, R.P., 2007. The evolution of the vertebrate metzincins; insights from Ciona intestinalis and Danio rerio. BMC Evol Biol 7, 63.

Hwang, W.Y., Fu, Y., Reyon, D., Maeder, M.L., Tsai, S.Q., Sander, J.D., Peterson, R.T., Yeh, J.R., Joung, J.K., 2013. Efficient genome editing in zebrafish using a CRISPR-Cas system. Nat Biotechnol 31, 227-229.

Irizarry, M.C., McNamara, M., Fedorchak, K., Hsiao, K., Hyman, B.T., 1997. APPSw transgenic mice develop age-related A beta deposits and neuropil abnormalities, but no neuronal loss in CA1. J Neuropathol Exp Neurol 56, 965-973.

Jagirdar, R., Fu, C.H., Park, J., Corbett, B.F., Seibt, F.M., Beierlein, M., Chin, J., 2021. Restoring activity in the thalamic reticular nucleus improves sleep architecture and reduces Abeta accumulation in mice. Sci Transl Med 13, eabh4284.

Jao, L. E., Wente, S. R., Chen, W. B. Efficient multiplex biallelic zebrafish genome editing using a CRISPR nuclease system. PNAS. 110, 13904-13909

Joshi, P., Liang, J.O., DiMonte, K., Sullivan, J., Pimplikar, S.W., 2009. Amyloid precursor protein is required for convergent-extension movements during Zebrafish development. Dev Biol 335, 1-11.

Ju, Y.E., Lucey, B.P., Holtzman, D.M., 2014. Sleep and Alzheimer disease pathology--a bidirectional relationship. Nat Rev Neurol 10, 115-119.

Ju, Y.S., Ooms, S.J., Sutphen, C., Macauley, S.L., Zangrilli, M.A., Jerome, G., Fagan, A.M., Mignot, E., Zempel, J.M., Claassen, J., Holtzman, D.M., 2017. Slow wave sleep disruption increases cerebrospinal fluid amyloid-beta levels. Brain 140, 2104-2111.

Jyoti, A., Plano, A., Riedel, G., Platt, B., 2010. EEG, activity, and sleep architecture in a transgenic AbetaPPswe/PSEN1A246E Alzheimer's disease mouse. J Alzheimers Dis 22, 873-887.

Kamenetz, F., Tomita, T., Hsieh, H., Seabrook, G., Borchelt, D., Iwatsubo, T., Sisodia, S., Malinow, R., 2003. APP processing and synaptic function. Neuron 37, 925-937.

Kang, J., Lemaire, H.G., Unterbeck, A., Salbaum, J.M., Masters, C.L., Grzeschik, K.H., Multhaup, G., Beyreuther, K., Muller-Hill, B., 1987. The precursor of Alzheimer's disease amyloid A4 protein resembles a cell-surface receptor. Nature 325, 733-736.

Kang, J.E., Lim, M.M., Bateman, R.J., Lee, J.J., Smyth, L.P., Cirrito, J.R., Fujiki, N., Nishino, S., Holtzman, D.M., 2009. Amyloid-beta dynamics are regulated by orexin and the sleep-wake cycle. Science 326, 1005-1007.

Kanyo, R., Leighton, P.L.A., Neil, G.J., Locskai, L.F., Allison, W.T., 2020. Amyloid-beta precursor protein mutant zebrafish exhibit seizure susceptibility that depends on prion protein. Exp Neurol 328, 113283.

Kollarik, S., Moreira, C.G., Dias, I., Bimbiryte, D., Miladinovic, D., Buhmann, J.M., Baumann, C.R., Noain, D., 2021. Natural age-related sleep-wake alterations onset prematurely in the Tg2576 mouse model of Alzheimer's disease. bioRxiv, 2021.2010.2025.465747.

Lechtreck, K.F., Delmotte, P., Robinson, M.L., Sanderson, M.J., Witman, G.B., 2008. Mutations in Hydin impair ciliary motility in mice. J Cell Biol 180, 633-643.

Leimer, U., Lun, K., Romig, H., Walter, J., Grunberg, J., Brand, M., Haass, C., 1999. Zebrafish (Danio rerio) presenilin promotes aberrant amyloid beta-peptide production and requires a critical aspartate residue for its function in amyloidogenesis. Biochemistry-Us 38, 13602-13609.

Li, Z.W., Stark, G., Gotz, J., Rulicke, T., Gschwind, M., Huber, G., Muller, U., Weissmann, C., 1996. Generation of mice with a 200-kb amyloid precursor protein gene deletion by Cre recombinase-mediated site-specific recombination in embryonic stem cells (vol 93, pg 6158, 1996). P Natl Acad Sci USA 93, 12052-12052.

Lim, A.S., Ellison, B.A., Wang, J.L., Yu, L., Schneider, J.A., Buchman, A.S., Bennett, D.A., Saper, C.B., 2014. Sleep is related to neuron numbers in the ventrolateral preoptic/intermediate nucleus in older adults with and without Alzheimer's disease. Brain 137, 2847-2861.

Lim, A.S., Kowgier, M., Yu, L., Buchman, A.S., Bennett, D.A., 2013. Sleep Fragmentation and the Risk of Incident Alzheimer's Disease and Cognitive Decline in Older Persons. Sleep 36, 1027-1032.

Loewenstein, R.J., Weingartner, H., Gillin, J.C., Kaye, W., Ebert, M., Mendelson, W.B., 1982. Disturbances of sleep and cognitive functioning in patients with dementia. Neurobiol Aging 3, 371-377.

Luna, S., Cameron, D.J., Ethell, D.W., 2013. Amyloid-beta and APP deficiencies cause severe cerebrovascular defects: important work for an old villain. PLoS One 8, e75052.

Magara, F., Muller, U., Li, Z.W., Lipp, H.P., Weissmann, C., Stagljar, M., Wolfer, D.P., 1999. Genetic background changes the pattern of forebrain commissure defects in transgenic mice underexpressing the beta-amyloid-precursor protein. P Natl Acad Sci USA 96, 4656-4661.

Manaye, K.F., Mouton, P.R., Xu, G., Drew, A., Lei, D.L., Sharma, Y., Rebeck, G.W., Turner, S., 2013. Age-related loss of noradrenergic neurons in the brains of triple transgenic mice. Age (Dordr) 35, 139-147.

Meeker, N.D., Hutchinson, S.A., Ho, L., Trede, N.S., 2007. Method for isolation of PCR-ready genomic DNA from zebrafish tissues. Biotechniques 43, 610, 612, 614.

Montague, T.G., Cruz, J.M., Gagnon, J.A., Church, G.M., Valen, E., 2014. CHOPCHOP: a CRISPR/Cas9 and TALEN web tool for genome editing. Nucleic Acids Res 42, W401-407.

Muller, U., Cristina, N., Li, Z.W., Wolfer, D.P., Lipp, H.P., Rulicke, T., Brandner, S., Aguzzi, A., Weissmann, C., 1994. Behavioral and Anatomical Deficits in Mice Homozygous for a Modified Beta-Amyloid Precursor Protein Gene. Cell 79, 755-765.

Musa, A., Lehrach, H., Russo, V.A., 2001. Distinct expression patterns of two zebrafish homologues of the human APP gene during embryonic development. Dev Genes Evol 211, 563-567.

Muto, V., Koshmanova, E., Ghaemmaghami, P., Jaspar, M., Meyer, C., Elansary, M., Van Egroo, M., Chylinski, D., Berthomier, C., Brandewinder, M., Mouraux, C., Schmidt, C., Hammad, G., Coppieters, W., Ahariz, N., Degueldre, C., Luxen, A., Salmon, E., Phillips, C., Archer, S.N., Yengo, L., Byrne, E., Collette, F., Georges, M., Dijk, D.J., Maquet, P., Visscher, P.M., Vandewalle, G., 2021. Alzheimer's disease genetic risk and sleep phenotypes in healthy young men: association with more slow waves and daytime sleepiness. Sleep 44.

Nalivaeva, N.N., Turner, A.J., 2013. The amyloid precursor protein: a biochemical enigma in brain development, function and disease. FEBS Lett 587, 2046-2054.

Ozcan, G.G., Lim, S., Leighton, P., Allison, W.T., Rihel, J., 2020. Sleep is bi-directionally modified by amyloid beta oligomers. Elife 9.

Pasquier, J., Cabau, C., Nguyen, T., Jouanno, E., Severac, D., Braasch, I., Journot, L., Pontarotti, P., Klopp, C., Postlethwait, J.H., Guiguen, Y., Bobe, J., 2016. Gene evolution and gene expression after whole genome duplication in fish: the PhyloFish database. Bmc Genomics 17.

Platt, B., Drever, B., Koss, D., Stoppelkamp, S., Jyoti, A., Plano, A., Utan, A., Merrick, G., Ryan, D., Melis, V., Wan, H., Mingarelli, M., Porcu, E., Scrocchi, L., Welch, A., Riedel, G., 2011. Abnormal cognition, sleep, EEG and brain metabolism in a novel knock-in Alzheimer mouse, PLB1. PLoS One 6, e27068.

Prinz, P.N., Vitaliano, P.P., Vitiello, M.V., Bokan, J., Raskind, M., Peskind, E., Gerber, C., 1982. Sleep, EEG and mental function changes in senile dementia of the Alzheimer's type. Neurobiol Aging 3, 361-370.

Prober, D.A., Rihel, J., Onah, A.A., Sung, R.J., Schier, A.F., 2006. Hypocretin/orexin overexpression induces an insomnia-like phenotype in zebrafish. J Neurosci 26, 13400-13410.

Reichert, S., Pavon Arocas, O., Rihel, J., 2019. The Neuropeptide Galanin Is Required for Homeostatic Rebound Sleep following Increased Neuronal Activity. Neuron 104, 370-384 e375.

Reyon, D., Maeder, M. L., Khayter, C., Tsai, S. Q., Foley, J. E. ,Sander, J. D., Joung, J. K. 2013 Engineering customized TALE nucleases (TALENs) and TALE

transcription factors by fast ligation-based automatable solid-phase high-throughput (FLASH) assembly,12, 12-16

Rihel, J., Prober, D.A., Arvanites, A., Lam, K., Zimmerman, S., Jang, S., Haggarty, S.J., Kokel, D., Rubin, L.L., Peterson, R.T., Schier, A.F., 2010. Zebrafish behavioral profiling links drugs to biological targets and rest/wake regulation. Science 327, 348-351.

Roh, J.H., Huang, Y., Bero, A.W., Kasten, T., Stewart, F.R., Bateman, R.J., Holtzman, D.M., 2012. Disruption of the sleep-wake cycle and diurnal fluctuation of beta-amyloid in mice with Alzheimer's disease pathology. Sci Transl Med 4, 150ra122.

Sager, J.J., Bai, Q., Burton, E.A., 2010. Transgenic zebrafish models of neurodegenerative diseases. Brain Struct Funct 214, 285-302.

Sander, J.D., Cade, L., Khayter, C., Reyon, D., Peterson, R.T., Joung, J.K., Yeh, J.R., 2011. Targeted gene disruption in somatic zebrafish cells using engineered TALENs. Nat Biotechnol 29, 697-698.

Sander, J.D., Zaback, P., Joung, J.K., Voytas, D.F., Dobbs, D., 2007. Zinc Finger Targeter (ZiFiT): an engineered zinc finger/target site design tool. Nucleic Acids Res 35, W599-605.

Seabrook, G.R., Smith, D.W., Bowery, B.J., Easter, A., Reynolds, T., Fitzjohn, S.M., Morton, R.A., Zheng, H., Dawson, G.R., Sirinathsinghji, D.J.S., Davies, C.H., Collingridge, G.L., Hill, R.G., 1999. Mechanisms contributing to the deficits in hippocampal synaptic plasticity in mice lacking amyloid precursor protein. Neuropharmacology 38, 349-359.

Sethi, M., Joshi, S.S., Webb, R.L., Beckett, T.L., Donohue, K.D., Murphy, M.P., O'Hara, B.F., Duncan, M.J., 2015. Increased fragmentation of sleep-wake cycles in the 5XFAD mouse model of Alzheimer's disease. Neuroscience 290, 80-89.

Seugnet, L., Suzuki, Y., Merlin, G., Gottschalk, L., Duntley, S. P., Shaw, P. J. 2011 Notch signaling modulates sleep homeostasis and learning after sleep deprivation in Drosophila. Curreent Biology 21, 835-840

Shokri-Kojori, E., Wang, G.J., Wiers, C.E., Demiral, S.B., Guo, M., Kim, S.W., Lindgren, E., Ramirez, V., Zehra, A., Freeman, C., Miller, G., Manza, P., Srivastava, T., De Santi, S., Tomasi, D., Benveniste, H., Volkow, N.D., 2018. beta-Amyloid accumulation in the human brain after one night of sleep deprivation. Proc Natl Acad Sci U S A 115, 4483-4488.

Song, P., Pimplikar, S.W., 2012. Knockdown of amyloid precursor protein in zebrafish causes defects in motor axon outgrowth. PLoS One 7, e34209.

Spira, A.P., An, Y., Wu, M.N., Owusu, J.T., Simonsick, E.M., Bilgel, M., Ferrucci, L., Wong, D.F., Resnick, S.M., 2018. Excessive daytime sleepiness and napping in

cognitively normal adults: associations with subsequent amyloid deposition measured by PiB PET. Sleep 41.

Steinbach, J.P., Muller, U., Leist, M., Li, Z.W., Nicotera, P., Aguzzi, A., 1998. Hypersensitivity to seizures in beta-amyloid precursor protein deficient mice. Cell Death Differ 5, 858-866.

Sterniczuk, R., Antle, M.C., Laferla, F.M., Dyck, R.H., 2010. Characterization of the 3xTg-AD mouse model of Alzheimer's disease: part 2. Behavioral and cognitive changes. Brain Res 1348, 149-155.

Sterniczuk, R., Theou, O., Rusak, B., Rockwood, K., 2013. Sleep disturbance is associated with incident dementia and mortality. Curr Alzheimer Res 10, 767-775. Tanzi, R.E., McClatchey, A.I., Lamperti, E.D., Villa-Komaroff, L., Gusella, J.F., Neve, R.L., 1988. Protease inhibitor domain encoded by an amyloid protein precursor mRNA associated with Alzheimer's disease. Nature 331, 528-530.

Thisse, C., Thisse, B., 2008. High-resolution in situ hybridization to whole-mount zebrafish embryos. Nat Protoc 3, 59-69.

Tremml, P., Lipp, H.P., Muller, U., Ricceri, L., Wolfer, D.P., 1998. Neurobehavioral development, adult openfield exploration and swimming navigation learning in mice with a modified beta-amyloid precursor protein gene. Behav Brain Res 95, 65-76. van Bebber, F., Hruscha, A., Willem, M., Schmid, B., Haass, C., 2013. Loss of Bace2 in zebrafish affects melanocyte migration and is distinct from Bace1 knock out phenotypes. Journal of Neurochemistry 127, 471-481.

Vitiello, M.V., Prinz, P.N., Williams, D.E., Frommlet, M.S., Ries, R.K., 1990. Sleep disturbances in patients with mild-stage Alzheimer's disease. J Gerontol 45, M131-138.

Wang, J., Ikonen, S., Gurevicius, K., van Groen, T., Tanila, H., 2002. Alteration of cortical EEG in mice carrying mutated human APP transgene. Brain Res 943, 181-190.

Weidemann, A., Konig, G., Bunke, D., Fischer, P., Salbaum, J.M., Masters, C.L., Beyreuther, K., 1989. Identification, biogenesis, and localization of precursors of Alzheimer's disease A4 amyloid protein. Cell 57, 115-126.

White, A.R., Multhaup, G., Maher, F., Bellingham, S., Camakaris, J., Zheng, H., Bush, A.I., Beyreuther, K., Masters, C.L., Cappai, R., 1999. The Alzheimer's disease amyloid precursor protein modulates copper-induced toxicity and oxidative stress in primary neuronal cultures. Journal of Neuroscience 19, 9170-9179.

Zhao, B., Liu, P., Wei, M., Li, Y., Liu, J., Ma, L., Shang, S., Jiang, Y., Huo, K., Wang, J., Qu, Q., 2019. Chronic Sleep Restriction Induces Abeta Accumulation by Disrupting the Balance of Abeta Production and Clearance in Rats. Neurochem Res 44, 859-873.

Zheng, H., Jiang, M.H., Trumbauer, M.E., Sirinathsinghji, D.J.S., Hopkins, R., Smith, D.W., Heavens, R.P., Dawson, G.R., Boyce, S., Conner, M.W., Stevens, K.A., Slunt, H.H., Sisodia, S.S., Chen, H.Y., Vanderploeg, L.H.T., 1995. Beta-Amyloid Precursor Protein-Deficient Mice Show Reactive Gliosis and Decreased Locomotor-Activity. Cell 81, 525-531.

FIGURE LEGENDS:

Figure 1. App gene organisation and expression in zebrafish

A) Zebrafish have two *App* orthologs, *appa* and *appb* in zebrafish. Appa contains the Kunitz type protease inhibitor (KPI) domain and thus has a similar gene organization to the human APP770 isoform. Zebrafish Appb lacks the KPI domain, similar to the brain enriched human APP695 isoform. Both Appa and Appb have the known functional App domains, including the Heparin binding domain (HBD), Copper binding domain (CuBD), extracellular E2 domain (E2), the conserved YENTPY motif, and Aβ region **B)** Alignment of Aβ regions of zebrafish Appa and Appb to human APP695 and APP770 shows high conservation including the proteolytic cleavage sites (indicated with black arrows); α-secretase cleavage site (α), β-secretase cleavage site (β), γ-secretase cleavage sites (γ) and ε-cleavage sites (ε). Black, dark grey, and light grey boxes indicate strictly, highly, and moderately conserved amino acid residues, respectively. **C)** CRISPR/Cas9 targeting of zebrafish *appa* resulted in a 5 bp deletion. The predicted translation of *appa*^{Δ5} leads to a premature stop codon within the Aβ region. TALEN targeting of zebrafish *appb* resulted in a 14 bp deletion and 4 bp insertion (red). The predicted translation of *appb*$^{Δ14+4}$ leads to a frameshift and a premature stop codon. **D)** As detected by ISH, *appa* and *appb* are both expressed in many larval brain areas at 5 days post fertilization (dpf) (left panel) D = dorsal, A=Anterior, L = Left. **E)** *appb* is expressed as early as the 1- to 8- cell stages, indicating that it is maternally deposited.

Figure 2. *appa*Δ5 mutants have reduced day waking activity but no sleep phenotype

A) Exemplar 40 hr traces of average waking activity from 5-7 dpf taken from a single experiment of *appa* mutants (*appa*$^{Δ5/Δ5}$), heterozygous (*appa*$^{Δ5/+}$), and wild type (*appa*$^{+/+}$)

siblings. Each line and shaded ribbon show the mean ± SEM. **B)** Day waking activity and **C)** Night waking activity larvae from an $appa^{\Delta5/+}$ incross, normalized to $appa^{+/+}$. **D)** Exemplar 48 hr traces of average sleep for the same experiment shown in A. **E**) Day sleep and **F**) Night sleep for larvae from an $appa^{\Delta5/+}$ incross, normalized to $appa^{+/+}$. **B,C,E,F)** Data combined across N=5 experiments. At top, each animal (dots) is normalized to the mean of experimentally-matched $appa^{+/+}$. Error bars indicate ± SEM. At bottom, the effect size ± 95% confidence interval are shown. $^{ns}p>0.05$, $^*p≤0.05$, Kruskal Wallis with Tukey's post-hoc test. n = the number of larvae.

Supplemental Figure 2-1. *appa* Δ5 mutants have no sleep phenotype

A) Day sleep bout length, **B)** Night sleep bout length **C)** Day sleep bout number, **D)** Night sleep bout number for larvae from an $appa^{\Delta5/+}$ incross. Each animal (dots) is normalized to the mean of $appa^{+/+}$ siblings. **A-D)** Data combined across N=5 experiments. Error bars indicate ± SEM. At bottom, the effect size ± 95% confidence interval are shown. $^{ns}p>0.05$ Kruskal Wallis with Tukey's post-hoc test. n = the number of larvae.

Figure 3. *appb* mutants have shorter sleep bouts across the day-night cycle

A) Exemplar 48 hr traces of average waking activity from 5-7 dpf taken from a single experiment of *appb* mutants ($appb^{-/-}$), heterozygous ($appb^{+/-}$), and wild type ($appb^{+/+}$) siblings. Each line and shaded ribbon show the mean ± SEM. **B)** Day waking activity, **C)** Night waking activity, normalized to $appb^{+/+}$ siblings combined across N=5 independent experiments. **D)** Average sleep for the same experiment shown in A. **E)** Day sleep, **F)** Night sleep, **G)** Day sleep bout length, **H)** Night sleep bout length, **I)** Day sleep bout number, and **J)** Night sleep bout number normalized to $appb^{+/+}$ siblings combined across N=5 independent experiments. **B-C, E-J)** At top, each animal (dots) is normalized to the mean of their experimentally-matched $appb^{+/+}$ data. At bottom, the effect size ± the 95% confidence interval relative to $appb^{+/+}$ are shown. $^{ns}p>0.05$, $^*p≤0.05$, $^{**}p≤0.01$, Kruskal-Wallis followed by Tukey's test. n = the number of larvae.

33

Figure 4. *Pharmacological blockade of y-secretase reduces sleep at night by decreasing sleep bout length*

A) Exemplar 48 hr traces of average waking activity from 5-7 dpf taken from a single experiment of WT larvae exposed to 100 nM DAPT or DMSO vehicle. Each line and shaded ribbon show the mean ± SEM. **B)** Day average waking activity, **C)** Night average waking activity of WT larvae exposed to DAPT are normalized to larvae exposed to DMSO only. **D)** Average sleep for the same experiment shown in A. **E)** Day sleep, **F)** Night sleep, **G)** Day sleep bout length, **H)** Night sleep bout length, **I)** Day sleep bout number, and **J)** Night sleep bout number of WT larvae exposed to DAPT normalized to DMSO vehicle. **B,C, E-J)** data combined across N=4 independent experiments. Each dot represents an animal. At bottom, the effect size ± the 95% confidence interval relative to DMSO control is shown. $^{ns}p>0.05$, *$p≤0.05$ Kruskal-Wallis followed by Tukey's test. n = the number of larvae.

Figure 5. *Pharmacological blockade of y-secretase in appb$^{-/-}$ background does not alter sleep at night*

A) Exemplar 48 hr traces of average waking activity from 5-7 dpf taken from a single experiment of *appb$^{-/-}$* larvae exposed to 100 nM DAPT or DMSO vehicle. Each line and shaded ribbon show the mean ± SEM. **B)** Day average waking activity, **C)** Night average waking activity, and **D)** Average sleep for the same experiment shown in A. **E)** Night sleep, **F)** Night sleep bout number, and **G)** Night sleep bout length of *appb$^{-/-}$* larvae exposed to DAPT are normalized to the mean of *appb$^{-/-}$* larvae exposed to DMSO vehicle. **H)** Night sleep, and **I)** Night sleep bout lengths of *appb$^{-/-}$* or wild type larvae exposed to DAPT are normalized to the mean of the WT larvae with DMSO vehicle. The wild type data is replotted from Figure 4 and the *appb$^{-/-}$* data is replotted from Figure 5A-G. **B**,**C**,**E-I)** Each dot represents an animal; data is combined across N=4 independent experiments. At bottom, the effect size ± the 95% confidence interval relative to each genotype's DMSO control is shown. $^{ns}p>0.05$ Kruskal-Wallis followed by Tukey's test. n = the number of larvae. *$p≤0.05$,

p≤0.01, 2-way ANOVA (genotype X drug interaction). **H, I) The experiment in both genotypes was performed at the same time in the same behaviour boxes. n = the number of larvae.

Supplemental Figure 5-1. *Pharmacological blockade of y-secretase in appb^{-/-}*

background does not alter sleep during the day

A) Day sleep, **B)** Day sleep bout length **C)** Day sleep bout number of 5-7 dpf *appb^{-/-}* larvae exposed to 100 nM DAPT or DMSO vehicle. Each animal (dots) is normalized to the mean of *appb^{-/-}* DMSO control. **A-D)** Data combined across N=4 experiments. Error bars indicate ± SEM. At bottom, the effect size ± 95% confidence interval are shown. $^{ns}p>0.05$ Kruskal Wallis with Tukey's post-hoc test. n = the number of larvae.
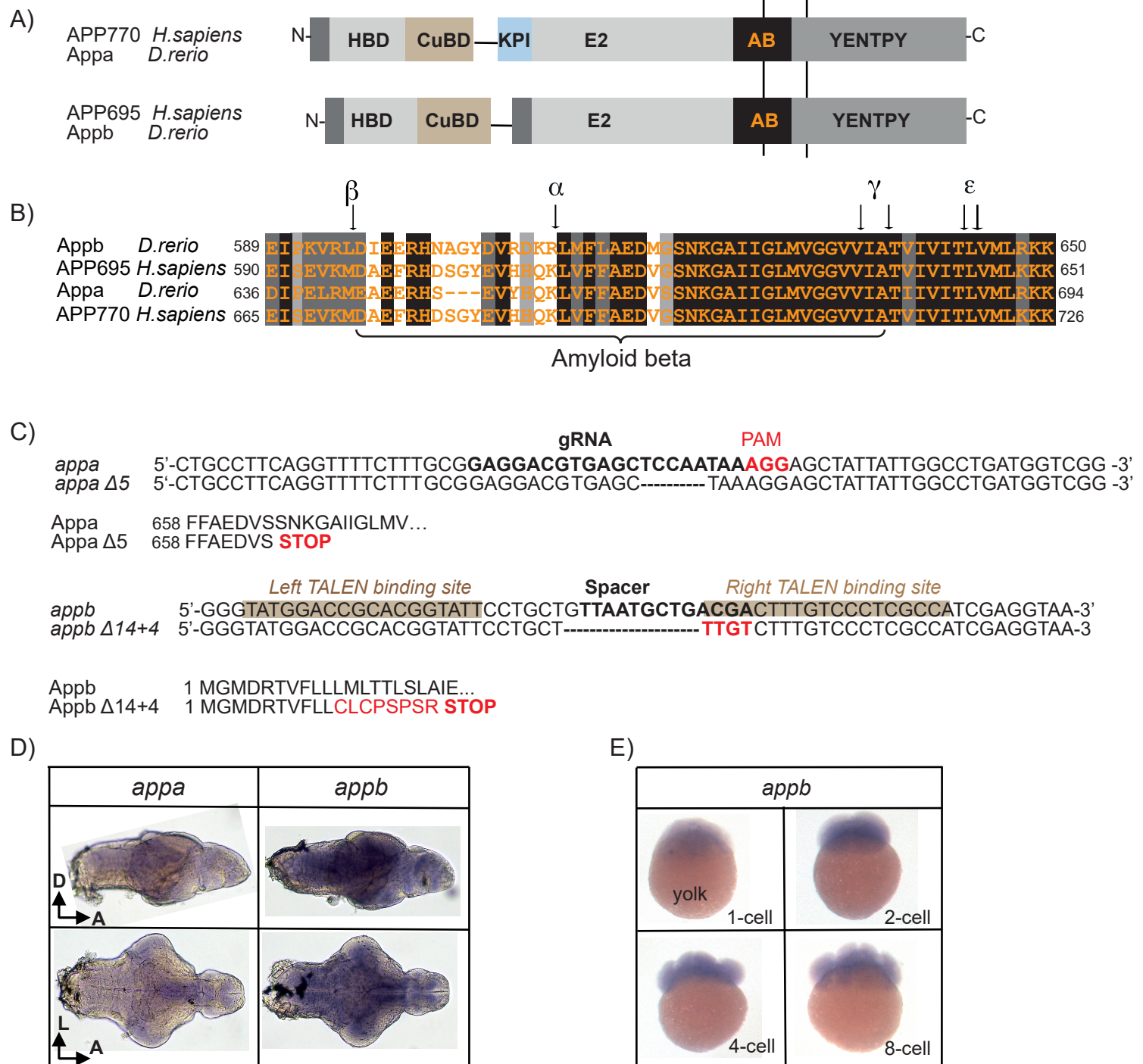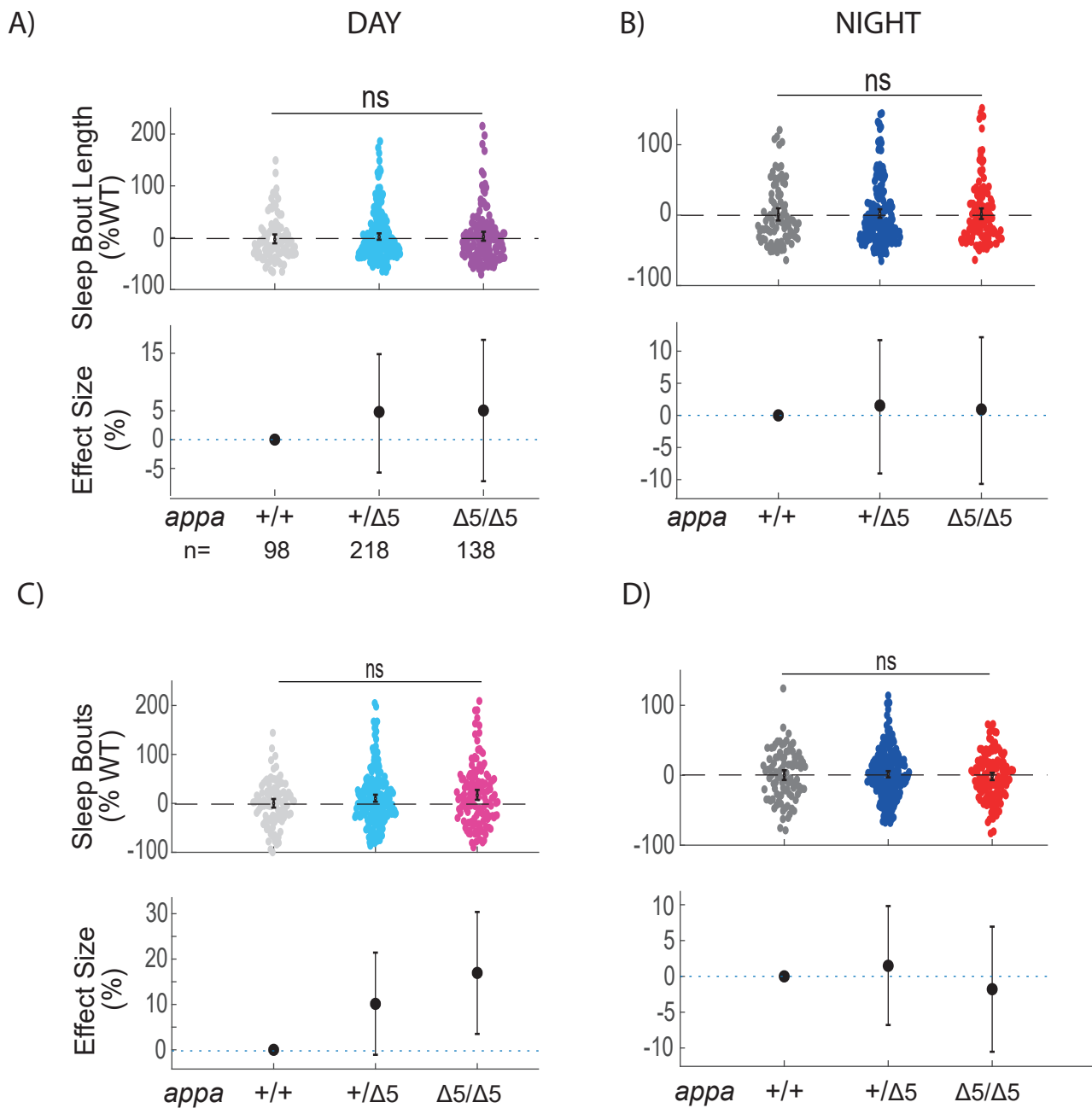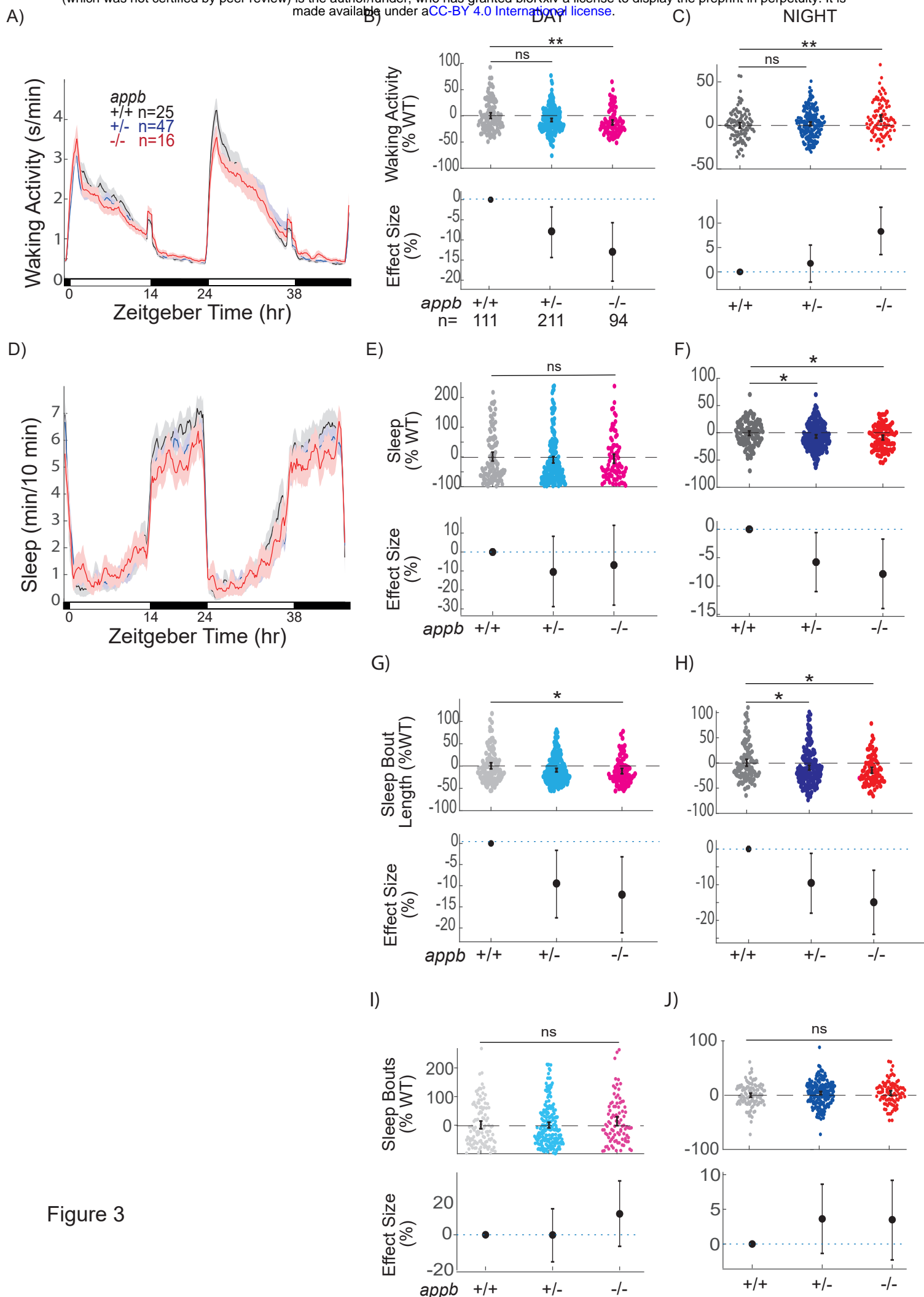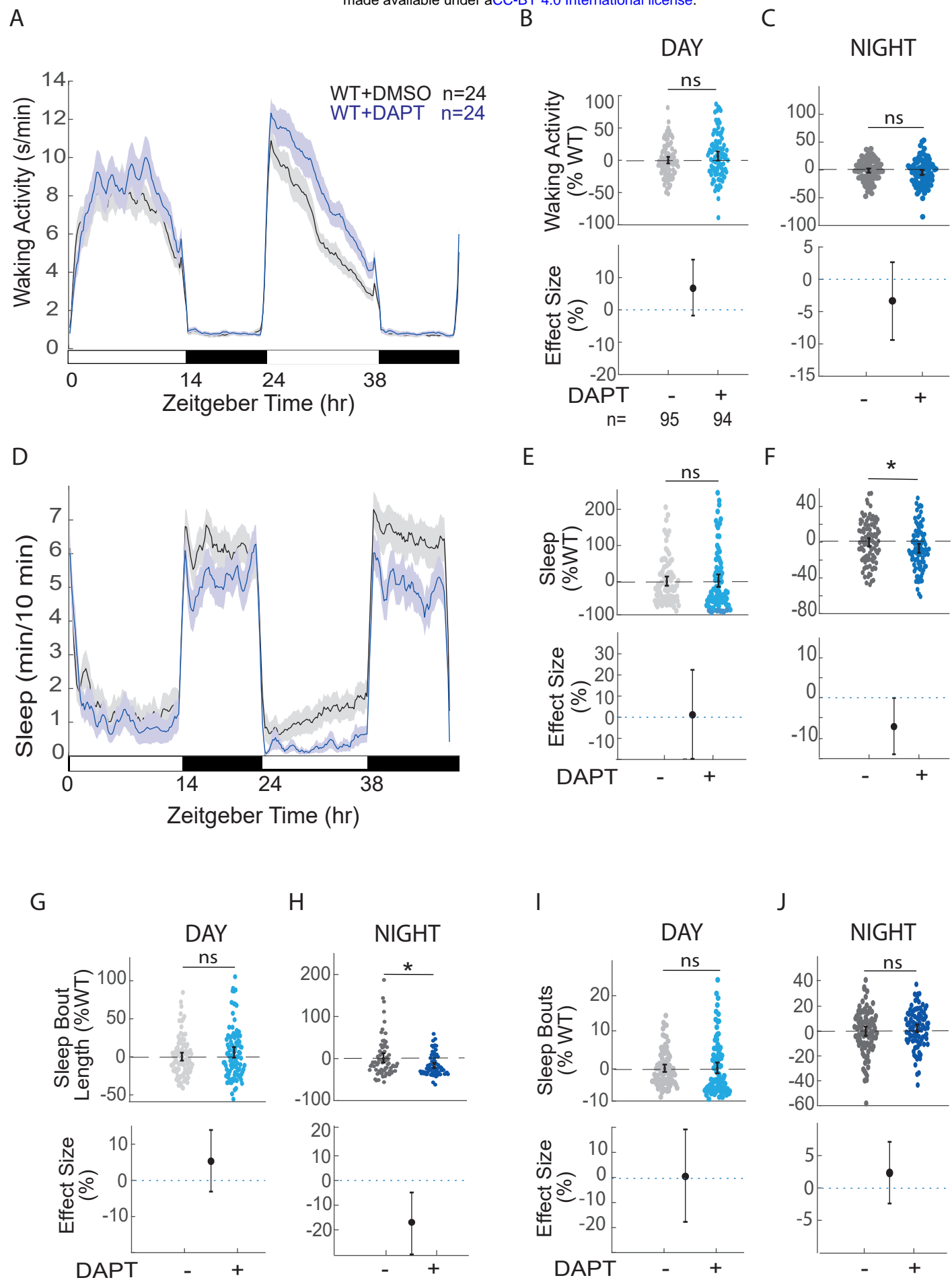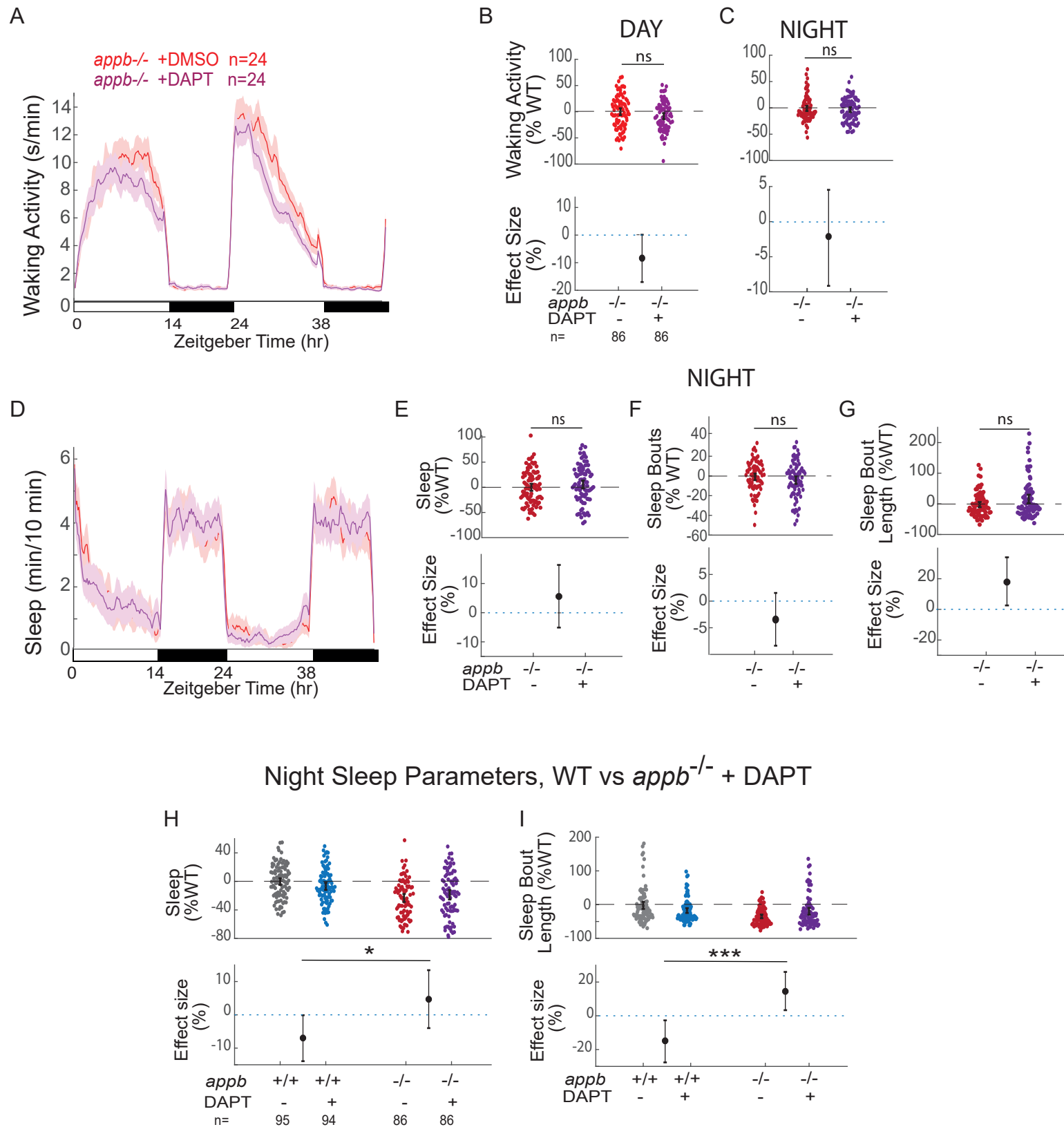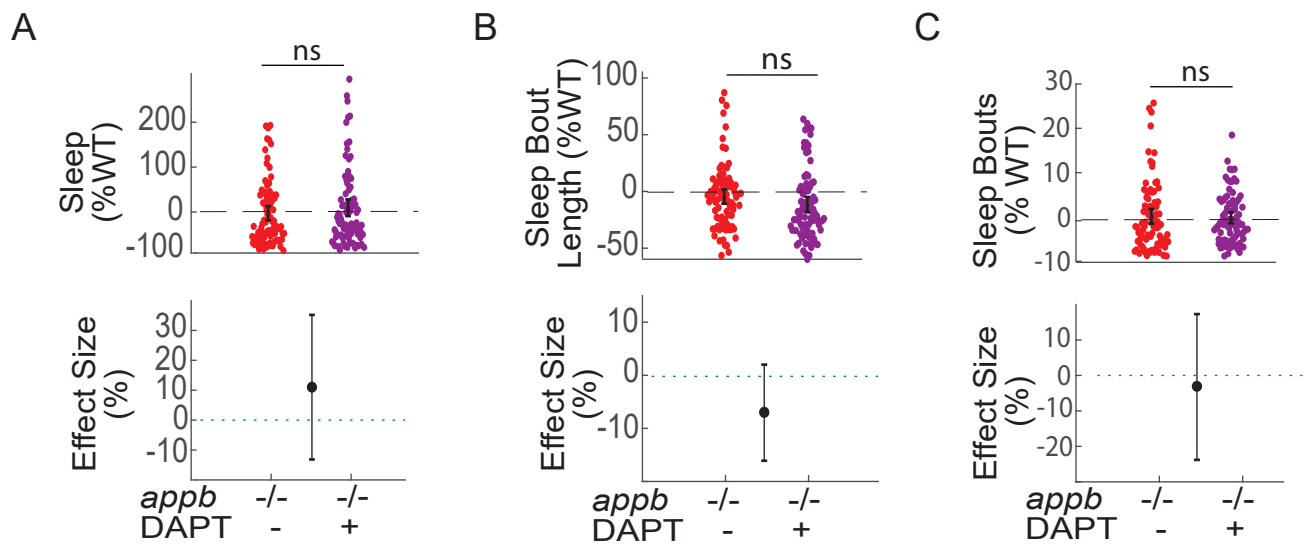
Figure 1
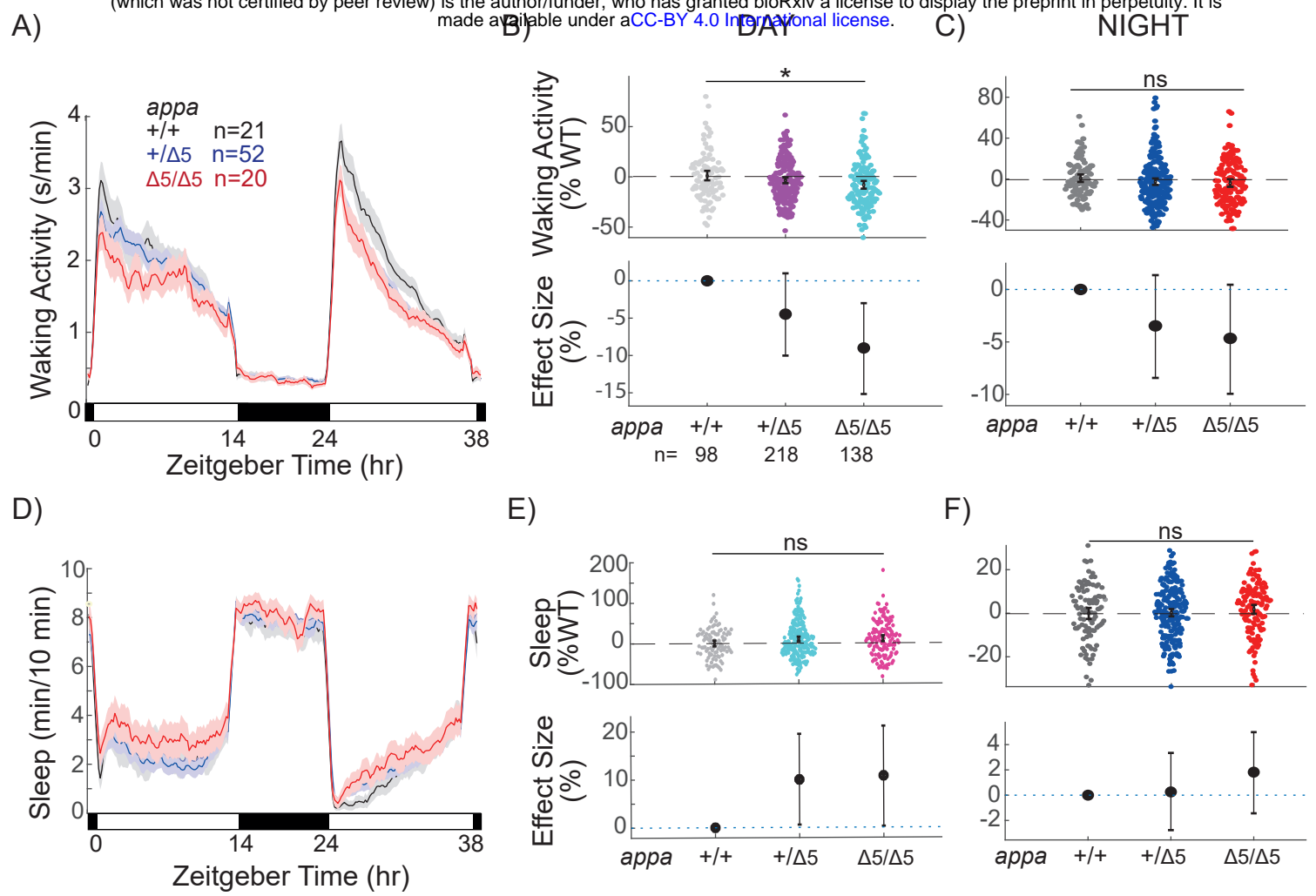
Figure 2

Figure Supplement 2-1

Figure 3

Figure 4

Figure 5

Day Sleep Parameters

Supplementary Figure 5-1